Available online at www.eccomasproceedia.org
Eccomas Proceedia COMPDYN (2017) 578-594

ECCOMAS
Proceedia

COMPDYN 2017
6th ECCOMAS Thematic Conference on
Computational Methods in Structural Dynamics and Earthquake Engineering
M. Papadrakakis, M. Fragiadakis (eds.)
Rhodes Island, Greece, 15–17 June 2017

PERFORMANCE-BASED DESIGN & ASSESSMENT OF SEISMICALLY ISOLATED BRIDGES WITH NON-LINEAR VISCOUS DAMPERS

Konstantinos I. Gkatzogias[1], **and Andreas J. Kappos**[1]

[1] Research Centre for Civil Engineering Structures, Dept. of Civil Eng., City, University of London
Northampton Square, London EC1V 0HB, UK
Konstantinos.Gkatzogias.1@city.ac.uk, Andreas.Kappos.1@city.ac.uk

Keywords: Bridges, Performance-Based Design & Assessment, Seismic Isolation, Non-linear Viscous Dampers, Non-linear Dynamic Analysis.

Abstract. *A performance-based design procedure is presented herein for seismically isolated bridges equipped with nonlinear viscous dampers (VDs). Accounting for multiple performance objectives, the proposed method initially identifies the critical hazard level and 'near-optimal' alternatives of the isolation system in terms of both economy and performance, based on the inelastic response of a single-degree-of-freedom system. By incorporating nonlinear response history analysis (NLRHA) of the multi-degree-of-freedom (MDOF) system in a number of successive design steps that correspond to different performance levels (PLs), it subsequently leads (in a non-iterative way) to a refinement of the initial design solution through the control of a broad range of material strains and deformations. The efficiency of the proposed design methodology is demonstrated by applying it to an actual bridge that was previously designed for ductile behaviour. Assessment of the design using NLRHA for spectrum-compatible motions indicates that the introduction of nonlinearity in viscous dampers can effectively reduce their size (i.e. reduced damper force demand) without significantly affecting the overall bridge response. Furthermore, enhanced seismic performance and cost reduction in the substructure design emerge, thus, rendering base-isolation an appealing design alternative.*

Peer-review under responsibility of the organizing committee of COMPDYN 2017.
doi: 10.7712/120117.5442.17855

1 INTRODUCTION

Viscous fluid damper (VD) devices employed in passive energy dissipation schemes as a means of mitigating seismic risk in structures are now well established; initially conceived as shock and vibration control units for military and aerospace technology purposes, their use was extended to civil structures in the early 1990s, gaining quickly widespread acceptance. Several methodologies have been proposed with regard to the seismic design of buildings equipped with VDs [1] varying from relatively simple to highly sophisticated ones; however, integrated design approaches addressing bridges equipped with both passive isolation and energy dissipation devices while aiming at a predefined structural response under a specific or, preferably, under multiple seismic hazard levels within a practical design context, have been fairly scarce and essentially based on linear equivalent-static/dynamic analysis (e.g. [2]). To estimate the peak inelastic response, such procedures usually employ equivalent linearisation techniques based on effective properties (i.e. stiffness and damping associated with maximum displacements); apart from the apparent requirement for iterative structural analysis, other related deficiencies may also arise, such as the inaccurate estimation of inelastic response due to the introduction of the ill-defined (i.e. non-physical) 'effective' isolation period [3] and the 'equivalent' damping ratio [4], the unreliable estimation of relative velocity required for the calculation of peak damper forces [5], and the inconsistent treatment of systems with non-classical (or non-proportional) damping matrices [4, 5].

In view of the previous considerations, the present study attempts to extend an existing rigorous performance-based design methodology for seismically isolated bridges [6] with a view to addressing nonlinear VDs, i.e. a feature of major importance in practical design due to the ability of nonlinear VDs to provide an effective line of defence against excessive damper forces caused by large velocity ground motions [7]. The suggested approach, called 'Deformation-Based Design' (Def-BD), originates from previous work presented by the authors on the seismic design of buildings [8] and bridges [9] relying on hysteretic energy dissipation through ductile behaviour. Def-BD in the form presented herein involves explicit design for multiple PLs and a broad range of design parameters, while providing the required tools for a direct comparative evaluation, at the early stages of design, of alternative isolation schemes that may consist of isolation and supplementary linear (LVD) or non-linear (NLVD) viscous damper devices, as well as combinations thereof. Detailed steps of the proposed Def-BD methodology and required modifications with regard to [6], aiming at considering the effect of nonlinearity of VDs, are presented in §2. Its efficiency is subsequently explored (§3) by applying it to an actual concrete bridge previously studied by the authors in the case of 'ductile pier' [9] and isolated [6] bridges. The suggested procedure and the resulting designs for two different isolation schemes focusing on the use of linear or non-linear VDs are then evaluated in the light of NLRHA using suites of natural and artificial spectrum-compatible motions. A comparison among the different designs, with emphasis on both economy and structural performance, is finally presented.

2 PROPOSED DEFORMATION-BASED DESIGN PROCEDURE

The target performance sought in Def-BD of seismically isolated bridges can be described with reference to member (e.g. pier and isolator) limit states and the associated seismic actions. For common bridges, a 'frequent' earthquake event (denoted EQII and having a return period T_r=50-200yrs, see [9] for EQI, not used herein) is associated with the 'operationality' limit state of isolators corresponding to non-disrupted service of the bridge, a 'rare' earthquake (EQIII: T_r=500-2500yrs) with quasi-elastic response of piers and minimal damage in the isolators without significant disruption of service, and a 'maximum considered' earthquake (EQIV:

T_r~2500yrs) with ultimate response of isolators, limited inelastic response of piers, and limited service of the bridge. The range of T_r coupled with each PL should be seen as indicative of the widely varying requirements prescribed in different codes for common bridges [9]; modification of the level of performance requirements and/or of T_r should be in order in the case of bridges of higher or lower importance. The target objectives are also in line with code specifications (e.g. [10]) regarding the necessity of limiting the inelastic response of the substructure, aiming at the proper performance of the isolation system, since it has been demonstrated [11], [12] that when inelastic action develops, the effectiveness of the isolation system may be reduced, resulting in larger deformation demands in the isolated structure. In the light of the previous consideration, controlled inelastic response of the piers (e.g. associated with spalling of concrete cover) is allowed only under EQIV. It is also noted, that a strict approach would require analysis of the seismically isolated bridge for three different PLs and two different sets of mechanical (i.e. lower bound (LB) and upper bound (UB) design properties (DPs)) of isolators and dampers, i.e. in total, six different sets of NLRHAs, each set consisting of seven (or more) pairs or triplets of accelerograms in an appropriate orientation. The following scheme reduces the required sets to three (i.e. one per each PL), noting however, that performing the 'full set' of analyses will in any case minimise the associated cost of the adopted isolation solution. For the sake of completeness all steps of the procedure (including those that are essentially the same with [6]) are summarized in the following.

2.1 Step 1: Preliminary design

Preliminary design in this step aims at the identification of the critical (in terms of economy and performance) PL and at a first 'near-optimal' estimation of the basic parameters of the isolation system, namely, its strength ($\overline{v}_0$), post-elastic stiffness (k_p) or isolation period (T_p), and damping ratio (ξ). $\overline{v}_0$ represents the ratio of $V_0/(mg)$, where V_0 is the shear capacity of the isolation system at zero displacement, m the isolated mass and g the acceleration of gravity. The 'near-optimal' isolation solution is defined herein as the one that results in 'near-minimum' peak total acceleration ($\ddot{U}_0$) of the superstructure while keeping within allowable limits the peak relative displacements (u_0) of the isolation system and the deformations of the substructure [13]; different approaches can be explored by duly exercising engineering judgement.

Both objectives of the preliminary design can be investigated either on the basis of an elastic (e.g. response spectrum) analysis by introducing an iterative equivalent-linearisation technique, similar to code-based approaches (e.g. [10]), or on the basis of 'design equations' that can provide direct estimates of u_0, $\ddot{U}_0$ as a function of ξ, η (i.e. strength normalised to seismic intensity [6]), and T_p, under different PLs associated with (code-based) target spectra of common frequency content but different intensity. The latter approach [6, 14], apart from being compatible with the framework of the 'deformation-based design' method (Def-BD) [9] has also the potential to deal with certain pitfalls of equivalent linearisation procedures (§1). To this end, 'design equations' in the form of Eqs. (1, 2), simplified in Table 1 for the case of elastomer-based isolators, were developed [6] by fitting a linear regression model to the normalised response of an isolated SDOF system under a suite of 10 artificial records generated [15] to fit a target spectrum with a frequency content corresponding to ground type 'C' [16] (Fig. 1). In general, 'design equations' can be extracted for code-prescribed target spectra and provided as ready-to-use tools. Although development of regression models is required in cases wherein spectra of different frequency content are adopted, the procedure can be easily automated based on a relatively small number of NLRHAs under spectrum compatible records. Strictly, the data of Table 1 refer to linear VDs; pending a future publication on the investigation of the effect of nonlinearity of VDs on the 'design equations', Eqs. (1, 2) are used herein to predict also the response of systems equipped with NLVDs, investigating their efficiency for a case study in §3.

$$u_0, \ddot{U}_0 = \frac{0.362 e^{\text{int}}}{2\pi g} \xi^{(\beta+\gamma \ln\eta+\delta \ln T_p)} \eta^{(1+\varepsilon+\zeta \ln\eta+\kappa \ln \text{T})} T_p^{(2+\lambda+\mu \ln T_p+\nu(\ln T_p)^2)} a_g \quad (1)$$

$$\eta = 4.31 \frac{\bar{v}_0 g}{a_g} \quad (2)$$

Case	*R*	*Int*	β	γ	δ	ε	ζ	κ	λ	μ	ν
η=0	u_0	5.245	-0.428	-	-	-	-	-	-1.194	0.797	-0.443
	$\ddot{U}_0$	8.952	-0.419	-	0.150	-	-	-	-2.266	-0.226	-
η=0.25-1.5	u_0	0.623	-0.178	0.097	-	-1.192	-0.095	-0.175	-1.100	-0.209	-
	$\ddot{U}_0$	4.769	-0.114	0.094	0.128	-0.754	0.153	0.255	-2.393	-	-

Table 1: Definition of 'design equations' for ground type C [16].

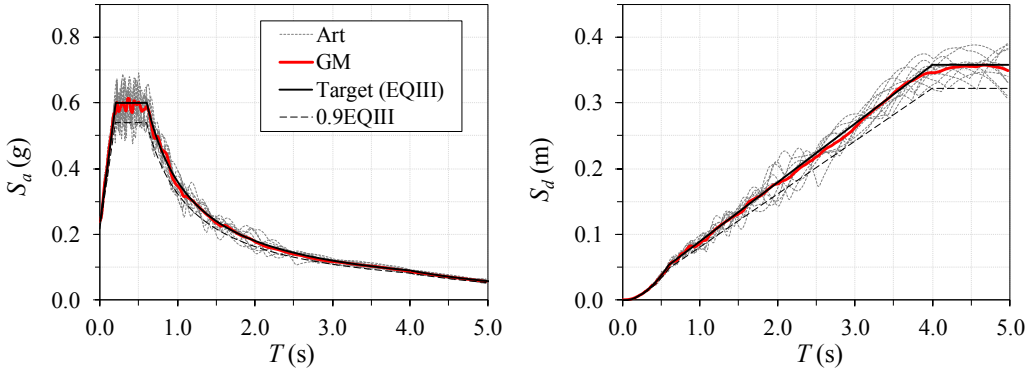

Figure 1: Spectral matching of the scaled median ('GM') response acceleration (left) and displacement (right) spectrum to the target spectrum (*PGA* of 0.21*g*) for a suite of artificial ('Art') recordings.

u_0 and $\ddot{U}_0$ inelastic spectra for the adopted EQIII and EQIV seismic intensities are first established by plotting Eq. (1) in a u_0-, $\ddot{U}_0$ vs $\bar{v}_0$ format (Fig. 2), facilitating the identification of isolation schemes (ξ, $\bar{v}_0$, T_p) with a 'near-optimal' performance under different earthquake intensities, and systems consisting of different isolation and energy dissipation devices. The above near-optimal selections for a given ξ are characterised by a constant value of η (i.e. the near-optimal η is independent of the seismic intensity) but in general correspond to different 'actual' isolation schemes due to the variation of $\bar{v}_0$ (see Eq. (2) and optimal selections denoted with blue in Fig. 2). Fig. 2, in agreement with other studies [17], indicates that when an isolated structural system designed for optimal performance under a 'rare' event (denoted as optEQIII) is subjected to stronger ground motions (e.g. EQIV), it results in suboptimal u_0 response compared to the displacement response of a system optimised for the increased hazard intensity (i.e. optEQIV). On the other hand, increased $\ddot{U}_0$ (and hence base shear) are obtained in the case of the optEQIV system when the latter is subjected to shorter return period events (e.g. EQIII). In design terms, the previous observation may be translated into an increased cost of isolators in the first case and an increased cost of reinforcing steel in the concrete piers in the second. In view of the previous remark, the decision on the reference hazard level to be used, or else, the earthquake intensity under which the isolation and energy dissipation system is near-optimally selected (i.e. EQIII or EQIV) should be made cautiously considering the divergence from optimal response (when the selected system is subjected to a different PL and/or different DPs) and

the relevant effect on economy and performance. It is noted that the variability of mechanical properties can be easily assessed provided that the relevant input (i.e. ξ, $\bar{v}_0$, T_p corresponding to LB- or UB-DP) is used in Eq. (1).

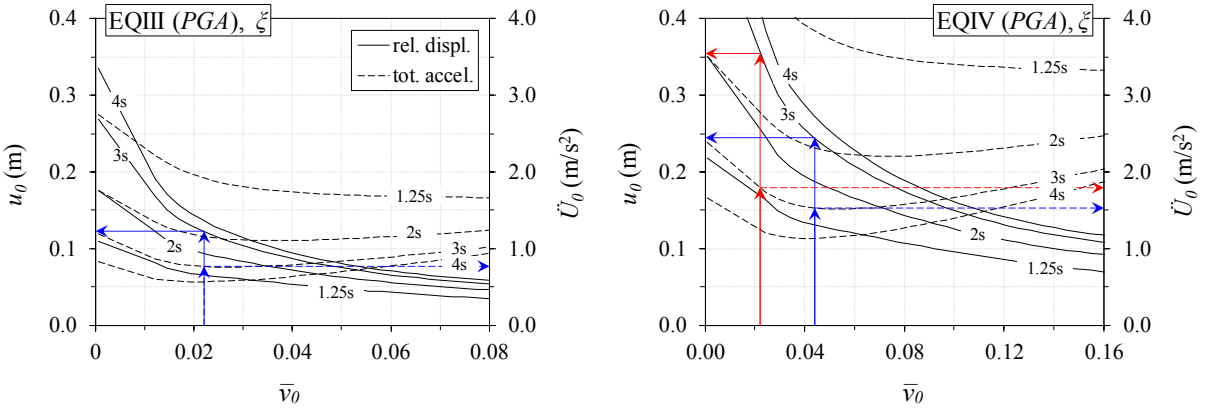

Figure 2: Direct peak response estimation of SDOF systems (m, ξ, T_p=3.0s, a=1.0) optimally designed (in blue) under EQIII (i.e. optEQIII) (left) and EQIV (i.e. optEQIV) (right), and corresponding response of optEQIII under EQIV (in red).

Eq. (1) and inelastic spectra in Fig. 2 can be also used in systems equipped with NLVDs by introducing an energy-equivalence approach [18]; the damping coefficients associated with viscous damping originating from elastomer-based isolators (c_e) and VDs (c_d) can be expressed by Eqs. (3, 4) where the equivalent viscous damping ratio ξ_d is used to describe the energy dissipation capacity of energy-equivalent VDs, the parameter a their nonlinearity ranging between zero (pure friction damping) and 1.0 (linear viscous damping), $\Gamma(\cdot)$ the gamma function, and ω_p the isolation frequency associated with k_p and T_p. u_0, required for the calculation of c_d when $a\neq1.0$, is defined herein as the peak displacement of the SDOF with an energy-equivalent linear VD of $\xi=\xi_e+\xi_d$ and a=1.

$$c_e = 2m\omega_p\xi_e, \quad c_d = \frac{2m\omega_p\xi_d\left(u_0\omega_p\right)^{1-a}}{f(\Gamma,\alpha)} \tag{3}$$

$$f\left(\Gamma,a\right) = \frac{2^{2+a}\Gamma^2\left(1+a/2\right)}{\pi\Gamma\left(2+\alpha\right)} \tag{4}$$

By approximating the response of a NLVD with an energy-equivalent LVD, Eq. (1) can provide direct estimates of response for systems of the same ξ but different a. However, since c_d depends on u_0, an iterative application of Eq. (1) will be required whenever the response of a near-optimal system is sought under a PL and/or design properties other than those used for its selection. The procedure is summarised as follows:

i. u_0 and $\ddot{U}_0$ response estimates of a near-optimally selected system (ξ, $\bar{v}_0$, T_p, and a<1) under the reference event are directly calculated from Eq. (1) assuming a=1;
ii. Assuming ξ_e=0.05 (in the case of elastomer-based isolators) and $\xi_d=\xi-\xi_e$, c_e and c_d are calculated under the reference event using Eq. (3) and u_0 from Step (*i*);
iii. c_e, c_d, $\bar{v}_0$, T_p are subsequently modified to account (if required) for the variability of DPs of devices, otherwise they remain constant (i.e. corresponding to specific devices);
iv. η and $\xi=\xi_e+\xi_d$ are calculated under the different PL and/or design properties by re-arranging Eqs. (2 & 3). Supposing that a<1.0, calculation of ξ requires the definition of an energy-

equivalent linear system which in turn will provide the unknown u_0 under the updated PL and/or DPs. An initial estimate of ξ can be derived from Eq. (3) by assuming a=1, thus uncoupling the above calculation from the displacement response;

v. Substituting ξ, η (from Step *iv*) and T_p (from Step *iii*) in Eq. (1) provides an initial estimate for u_0 and $\ddot{U}_0$ under the different PL and/or design properties.
vi. Once u_0 has been determined, Steps (*iv*) & (*v*) are repeated until all relevant design quantities (i.e. ξ, u_0 and $\ddot{U}_0$) have practically stabilised.

In cases of a=1.0, Step (*vi*) will be redundant (i.e. no iterations required, as in [6]), whereas the decision on the adopted reference event will have no effect on the system's optimal response in the special case of a=1.0 and η=0, due to the system's inherent linearity. The selection of a system with a 'near-optimal' performance may also encompass additional design constraints, such as, a target T_p, a maximum value of ξ or $\bar{v}_0$, and a target u_0, accounting for both economy and market availability of the selected dampers, isolators, and expansion/contraction joints. Note also that the decision on the type of devices required to materialise the selected system will normally follow the selection of ξ, η, T_p, apart from the case when specific restrictions apply. An example of the above procedure is presented in §3.

Selecting an isolation and energy dissipation system will result in a first estimation of the geometrical and mechanical (LB, UB) properties of devices to be used in subsequent steps, so long as, ξ, η, and T_p, of the selected system are properly distributed to a sufficient number of units located at the piers and abutments, accounting for the weight distribution of the deck to the substructure, and aiming at the minimisation of the eccentricity between the centre of stiffness of the substructure-isolation system and the centre of mass of the supported deck to mitigate torsional effects. Uniformity of the stiffness of piers with different height can be achieved to some extent by tailoring the isolator properties so that the bearing stiffness counterbalances the difference in pier stiffness [19]. Notwithstanding the importance of the previous factors, reliability and cost issues will normally dictate the above distribution, e.g. selection of two isolators per pier/abutment is the most reliable and cost-effective design solution in the case of box girder section decks [20], while identical devices are preferable in small-to-moderate bridges since the cost for testing of devices is minimised. It is worth noting that the constraint of maintaining classical normal modes (i.e. distribution of damping constants proportional to the lateral stiffness of the substructure) does not apply here due to the use of NLRHA, hence, optimal distributions of dampers may be explored [7].

Distribution of properties of the selected isolation system and determination of LB/UB-DPs of devices will also provide an estimate of the pier strength required to ensure the target performance under the selected reference event, i.e. quasi-elastic response of piers under EQIII or controlled inelastic response under EQIV. Regarding the second case, the strength at the pier ends should be established to retain the effectiveness of the isolation system under an 'extreme' event through proper consideration of the range within which the inelastic deformations should fall (associated with the degree of damage allowed under EQIV). To meet this objective, the procedure described in Step 1 of Def-BD for 'ductile pier' bridges [9], used to ensure that the bridge remains operational during and after EQII, can be fully implemented herein under EQIV without requiring an elastic analysis; pier column forces and chord rotations can be estimated from the maximum shear transferred through the isolator to the pier top and a proper estimation of the pier equivalent cantilever height (h_{eq}). The reader is referred to [9] for further details on the calculation of reduced design moments that are directly related to allowable deformations. In case the longitudinal reinforcement demand (ρ_l) is found to be less than the minimum requirement, reduction of cross sections is in order. An issue deserving some further consideration is that convergence of response quantities derived from Eq. (8) and the MDOF analysis in the following steps, depends on the substructure's stiffness (potentially involving limited inelastic

response) and inertial characteristics that are ignored in Step 1. Consideration of the latter parameters is deemed superfluous at this stage since subsequent steps of the method involve NLRHA of a detailed model of the bridge.

2.2 Step 2: 'Operationality' verifications

During this step a partially inelastic model (PIM) of the structure is set up, wherein hysteretic isolators and dampers are modelled as yielding and dashpot elements, respectively, with mechanical properties as defined in Step 1 based either on LB-DPs or UB-DPs or on both, as described in the following. In the same model, the remaining parts of the bridge are modelled as elastic members. The flexural stiffness of prestressed concrete deck elements is calculated assuming uncracked deck sections while reinforced concrete pier column stiffness should correspond either to yield (e.g. moment M vs curvature φ analysis of sections based on ρ_l estimated in Step 1) or to the gross section; pier stiffness under EQII is expected to have a minor effect on isolator deformations used in the following verifications. NLRHA of the PIM also requires the definition of a suite of ground motions, which, in a design context, should be compatible with the selected design spectrum. Selection and scaling of input motions can be performed according to the procedures described in [9]. The selected earthquake motions will be used for both this step and the following ones, and they should be properly scaled to the level associated with the PL considered; alternatively, different suites of motions can be established for each PL based on different selection criteria and shape of target spectra in a more refined approach that is expected to be more essential in the case of bridges of higher importance.

Verifications under the EQII event should be carried out in terms of both 'operationality' and 'structural performance' of the bridge, hence, design criteria in this PL should ensure both 'full' service of the bridge (i.e. no closure) and 'negligible' (or preferably no-) damage of the isolation and energy dissipation devices. The 'operationality' requirement can be satisfied by providing an adequate restoring capability, a design strategy common in most codes, by dictating the presence of devices that can inherently apply re-centring forces to the superstructure, thus preventing substantial residual displacements (u_{res}) after the seismic event and accumulation of displacements during a sequence of seismic events or under ground motion containing pulses, while allowing the prediction of displacement demand with less uncertainty [20]. The restoring capability should be assessed on the basis of design charts (e.g. [21, 22]) derived from statistical analysis of responses from a large number of NLRHAs since the absence of u_{res} in NLRHA results under few (e.g. 3–10) horizontal pairs of spectrum-compatible records is not always indicative of sufficient restoring capability.

In view of the previous remarks, the isolation system design should aim at 'full' service of the bridge at this PL (i.e. near-zero u_{res}) and at 'limited' service at the PL associated with EQIII. Engineering judgement will be required at this stage in defining allowable u_{res} values associated with the 'closure/non-closure' state of the bridge [6], noting that the capability of bilinear isolation systems is expected on average to be relatively lower for seismic motions involving small-to-moderate displacements and UB-DPs. A more stringent ('force-based') 'operationality' criterion under EQII can be the limitation of the isolation base shear below V_0 assuming UB-DPs; this will ensure zero u_{res} of the deck in the case of sliding bearings, and thus, 'full' serviceability of the bridge, but is more difficult to apply in lead rubber bearings due to the actual gradual transition from the elastic to the inelastic range of response (i.e. uncertainty with regard to the definition of the yield displacement u_y); nevertheless, the previous criterion can be applied by conservatively estimating u_y. Considering the requirement for 'negligible' damage of isolators, an upper limit of deformation (combined with an appropriate safety factor) corresponding to the yielding of the steel shims (e.g. shear strains due to lateral deformation γ_q lower than 1.0 [23]) should be applied in the case of elastomer-based isolators and LB-DPs.

Use of UB- or LB-DPs of devices during the analysis in this step, should be in order for the verification of 'force-based' (including restoring capability) or 'deformation-based' operationality criteria, respectively. In the (common) case wherein both types of criteria are involved, analysis should be based either on UB- or LB-DPs depending on the most critical one (see §3). Verifications associated with mechanical properties not accounted for in the analysis should be conducted using conservative estimates of the demand implicitly related to analysis results through proper modification factors; the latter can be calculated as the ratio of the relevant UB/LB design quantities derived from Eq. (1). Alternatively, the designer may opt to apply consecutively UB- and LB-DPs, in this and the following PLs, to ensure a minimum cost of the adopted isolation solution. If the adopted performance criteria are not satisfied, mechanical properties of devices should be modified without performing additional NLRHAs; conformity to the requirements of Step 1 (i.e. performance under the reference event) can be evaluated using Eq. (1). When the required modifications in this step do not satisfy the target performance set in Step 1, alternative (probably less economical) design options can be explored, such as adding sacrificial devices that can restrain the relative movement of the deck to the piers for the relatively low shear forces under EQII. In any case, operationality verifications at this step are not expected to be critical for piers, as the latter are designed for responding quasi-elastically up to the next PL.

2.3 Step 3: 'Minimal damage' verifications

During analysis in this step, the PIM of Step 2 should be used with pier stiffness corresponding to yield and UB-DPs of devices (as modified in Step 2). Verifications under a 'rare' event should ensure that the extent of damage is such that the bridge can be easily repaired after the earthquake without any significant disruption of service. Regarding the isolation system, the previous requirement can be expressed as an adequate restoring capability allowing for u_{res} that can result in a 'brief' closure of the bridge, and 'minimal' damage in the isolators (e.g. γ_q=1~1.5), both evaluated according to the previous step. Required modifications of the isolator mechanical properties should be evaluated based on the requirements of Steps 1 and 2; some additional control over the restoring capability requirements can be gained through the adjustment of the substructure stiffness (increase of pier stiffness will normally increase the relative deformation of the isolation system). The performance sought for the substructure at this PL refers to essentially elastic response of piers. When design for flexure is carried out in terms of design values of material strength (hence using commonly available design aids), pier moment and shears derived from analysis (based on mean values of strength) should be properly reduced similarly to Def-BD of 'ductile-pier' bridges [9]. The final ρ_l ratio should be selected by adopting the highest demand derived from Steps 1 and 3.

2.4 Step 4: 'Life-safety' verifications

Verification of deformations in both the isolation system and the substructure under EQIV constitutes the primary objective in this step. Adoption of LB-DPs during analysis, followed by an explicit calculation of the deformation demand in the isolation system, or adoption of UB-DPs, that will provide an accurate estimation of the deformations in the substructure, should be selected in accordance with the available capacity of substructure members and devices and the estimated response from Eq. (1). For example, if the estimated displacement demand of the isolators from Step 1 is close to the capacity of the devices selected in subsequent steps, it is preferable to adopt LB-DPs during the analysis under EQIV with a view to assessing accurately (through analysis) the deformation demand in the isolation system and implicitly (through modification factors) the pier deformation demand. The designer may also opt for analysing the

isolated bridge under both LB- and UB-DPs, ensuring that neither the devices nor the substructure members (piers) are overdesigned. In any case, pier strength and stiffness should be calculated from M-φ analysis using the ρ_l ratios determined in Step 3.

Verification of the 'near-optimal' performance sought in Step 1 and subsequently modified in Steps 2, 3 is of particular importance for the isolation system; the deformation capacity of isolation and energy dissipation devices should be checked for ultimate deformations (also accounting for residual displacements [22] so that the isolation system can sustain possible aftershocks), uplift, and stability. With regard to the piers, it should be verified that the deformation demand is consistent with the limit state values allowing for controlled inelastic response of piers under EQIV calculated using section analysis; detailing of piers for confinement, anchorages and lap splices, should be carried out with due consideration of the expected level of inelasticity [9]. Moreover, shear design of piers should be carried out for EQIV and UB-DPs. Finally, in case the characteristics of the selected isolation devices deviate from those of typical devices provided by the manufacturer, checking of stresses in reinforcing shims (internal plates) and design of end plates should also be performed during this step (e.g. [20])

3 CASE STUDY

To evaluate the efficiency of the proposed procedure, a 3-span bridge of total length L=99m was investigated (Fig. 3); the 10m wide prestressed concrete box girder deck has a 7% longitudinal slope and it is supported by two single-column piers of cylindrical section and heights of 5.9 and 7.9m. The deck rests on piers and abutments through isolators allowing movement of the deck in any direction. The bridge lies on firm soil and both piers and abutments have surface foundations (footings). The selected structure is similar to the T7 Overpass previously used by the authors as a case study of Def-BD for bridges of ductile behaviour [9]. Apart from the modification of the pier-to-deck connection (i.e. monolithic in T7), the clear height of the piers is reduced herein to accommodate the pier cap (height of 1.5m). For the sake of consistency and with a view to enabling a meaningful comparison with T7, certain design parameters were defined in line with [9]. In particular, EQIII was associated with the EC8 'Type 1' elastic spectrum (T_r=475 yrs) for a PGA of 0.21g, ground type 'C', and assuming the corner period marking the transition from the velocity-sensitive to the displacement-sensitive region of the target spectrum equal to T_D=4.0s (i.e. compatible with 'design equations' of Table 1 and in line with recent research findings [24]), whereas EQII and EQIV were selected as half and twice the spectrum of EQIII, respectively. Furthermore, the output of the Def-BD methodology in [9] regarding the geometry of the piers (i.e. D=1.2m) was used as a starting point, focusing on the transverse response of the bridge and ignoring SSI effects. Response-history analysis was carried out using Ruaumoko 3D [25].

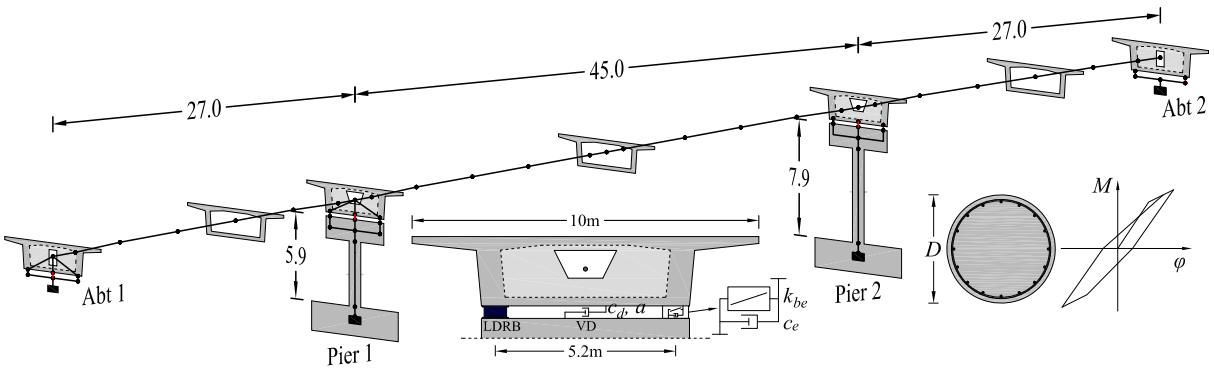

Figure 3: Configuration and modelling of studied bridge.

The focus in the following is on the design and assessment of two different isolation schemes that are representative of just a few of the available options and design criteria that can be explored; the adopted schemes are only differentiated with respect to the incorporation of linear or non-linear VDs, aiming at the investigation of the effect of nonlinearity of dampers (the reader should refer to [6] for additional isolation configurations). The efficiency of the adopted schemes within the examples of this study is evaluated using both approaches with regard to the variability of design properties of devices during design (i.e. 'reduced' and 'full' set of analyses according to §2); at the assessment stage safety checks are always performed for the element forces and displacement demands resulting from each possible combination of design properties (LB, UB) and PL.

Within Step 1, Eqs. (1, 2) were used to plot inelastic spectra in the form of Fig. 4 corresponding to different levels of seismic action (EQIII, EQIV) and an isolated deck mass (m) of 2545tn; similar spectra can be plotted for different combinations of ξ, η, T_p, and PGA representing different isolation schemes under various PLs. In Fig. 4, the $\ddot{U}(opt)$ curve represents a visualisation of the design criterion of minimum $\ddot{U}_0$ per T_p, while $u(opt)$ indicates the corresponding relative displacements of the isolation system. It should be noted that the abrupt change in the slope of the u_0, $\ddot{U}_0$ curves is due to the regression model adopted during the formulation of the 'design equations'; further refinement of the estimates requires the use of higher-order models that is deemed redundant since divergence from analysis results is evident only in the case of short isolation periods that are of little interest in bridge isolation applications. In Table 2, the estimated peak response of three alternative isolation schemes is presented, denoting with blue the response that corresponds to the reference event associated herein with LB-DPs and used to select the isolation scheme (i.e. EQIII in the upper part and EQIV in the lower part of the table), and with black, the corresponding response under a different PL, all derived from Eqs. (1, 2) according to the procedure described in §2.1. Response estimates are also provided for UB-DPs expected to yield the critical response quantities for the substructure elements; assumptions used in the calculation of DPs are provided later in this example.

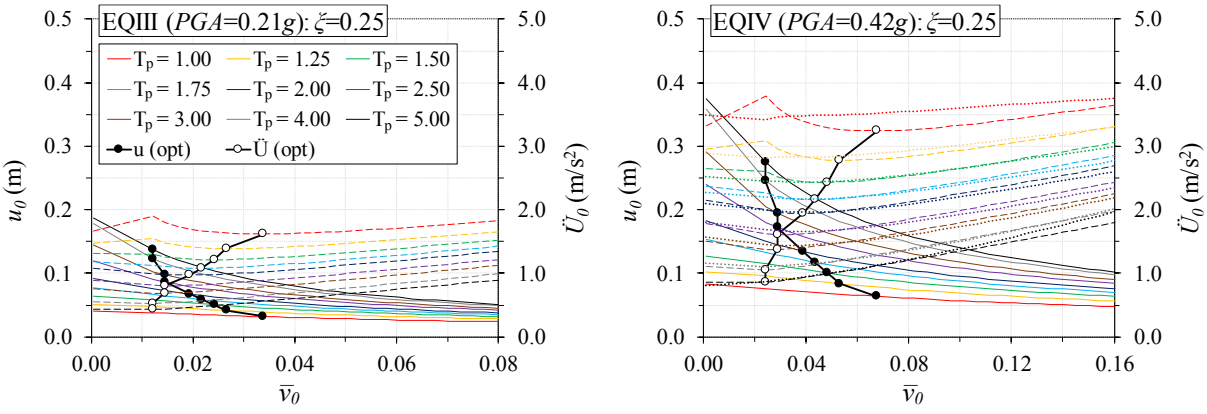

Figure 4: Peak relative displacements (u_0) (solid), total accelerations ($\ddot{U}_0$) (dashed), optimal peak total accelerations ($\ddot{U}opt$) and corresponding relative displacements ($uopt$) of deck under EQIII (left) and EQIV (right) predicted from 'design equations' (ξ=0.25). Dotted acceleration curves (right) represent NLRHA results.

Considering the last two columns of Table 2 where non-optimal responses are compared with their optimal counterparts, it is seen that when an isolated system with T_p=3.0s and optimally selected $\bar{v}_0$ under EQIII (No. 1.1) is subjected to EQIV, it develops higher u_0 (~41% for LB-DPs) and lower $\ddot{U}_0$ (~6% for UB-DPs) demand compared to the response of a system designed with the same ξ and T_p, but with $\bar{v}_0$ aiming at the minimisation of $\ddot{U}_0$ under EQIV (No. 1.2). On the other hand, an optEQIV system subjected to EQIII and UBDPs, develops ~39%

smaller u_0 (expected to have an adverse effect on the restoring capability) and ~24% larger $\ddot{U}_0$ demand compared to the optEQIII system. The decision on the reference event has no effect on a system of η=0 and a=1.0 (strictly, not optimally selected according to Fig. 4) due to its inherent linearity (No. 2.1, 2.2) in contrast to the case wherein nonlinearity in supplemental damping is introduced (a=0.2 in No. 3.1, 3.2). In fact, implementation of the iterative procedure described in §2.1 required to predict the response of a system with a<1.0 under PLs and/or DPs that are different from those used during its selection (in which case the response is assumed equal to that of a=1.0) yields smaller u_0 (~25%) and $\ddot{U}_0$ (~17%) when EQIV is set as the reference event.

No.	DP	$\bar{v}_0$	T_p (s)	ξ	η	u (m)	$\ddot{U}$ (m/s^2)	ξ	η	u (m)	$\ddot{U}$ (m/s^2)	Δu (%)	$\Delta\ddot{U}$ (%)
		opt EQIII		opt EQIII (1)				EQIV (2)				[(2) - (4)] / (4)	
1.1	LB	0.022	3.00	0.05	0.45	0.129	0.77	0.05	0.23	0.363	1.69	40.9	9.6
	UB	0.049	2.49	0.05	1.01	0.072	0.98	0.05	0.51	0.216	1.84	49.2	-6.2
(a=1)													
2.1	LB	0.001	2.50	0.25	0.01	0.120	0.89	0.25	0.01	0.240	1.78	0.0	0.0
	UB	0.001	2.07	0.27	0.01	0.092	1.01	0.27	0.01	0.183	2.03	0.0	0.0
(a=0.2)													
3.1	LB	0.001	2.50	0.25	0.01	0.120	0.89	0.15	0.01	0.302	2.07	26.1	16.5
	UB	0.001	2.07	0.29	0.01	0.089	0.99	0.17	0.01	0.227	2.37	27.4	19.5
		opt EQIV		EQIII (3)				opt EQIV (4)				[(3) - (1)] / (1)	
1.2	LB	0.044	3.00	0.05	0.90	0.086	0.83	0.05	0.45	0.258	1.54	-33.5	7.7
	UB	0.098	2.49	0.05	2.02	0.044	1.22	0.05	1.01	0.145	1.97	-38.8	23.6
LDRBs+LVDs (a=1)													
2.2	LB	0.001	2.50	0.25	0.01	0.120	0.89	0.25	0.01	0.240	1.78	0.0	0.0
	UB	0.001	2.07	0.27	0.01	0.092	1.01	0.27	0.01	0.183	2.03	0.0	0.0
LDRBs+NLVDs (a=0.2)													
3.2	LB	0.001	2.50	0.49	0.01	0.090	0.74	0.25	0.01	0.240	1.78	-24.8	-17.2
	UB	0.001	2.07	0.59	0.01	0.066	0.80	0.29	0.01	0.178	1.98	-25.7	-19.4

Table 2: Comparison of peak responses among SDOF systems optimised for different earthquake intensities

In general, the adopted approach should be based on the evaluation of data in the form of Table 2 for different isolation schemes accounting for both economy and market availability of materials and devices. Herein, EQIV was set as the reference event and two different isolation schemes characterised by ξ=0.25, $\bar{v}_0$ =0, and T_p=2.5s were investigated; the first materialised by low damping rubber bearings (LDRBs) and LVDs (No. 2.2 in Table 2), and the second by the combined use of LDRBs and non-linear VDs with a=0.2 (No. 3.2). The schemes were selected on the grounds that the distributed base shear ($m\ddot{U}_0$) to the piers results in pier reinforcement ρ_l larger than the minimum required while keeping u_0 of the deck below the maximum displacement obtained during the design of the bridge for ductile behaviour [9].

The required characteristics of isolation devices were defined by considering the properties of the isolation schemes in Table 2 under the reference event associated with LB-DPs. Due to the relatively small length of the studied bridge it was deemed appropriate to use 8 identical isolators (i.e. 2 per abutment/pier) and 4 identical VDs (i.e. 1 per abutment/pier); it is recalled that only the transverse response is addressed herein (normally, VDs will also be provided in the longitudinal direction). The diameter of the isolators (D_b) was defined assuming an allowable vertical stress $\sigma_{v,max}$=12MPa, while the required $k_p=4\pi^2 m/T_p^2$ of the isolation system was evenly distributed to all isolators ($k_{bp}=k_p/8$=2007 kN/m) providing the required height of the elastomer as $t_R=\pi G D_b^2/(4k_{bp})$, where G is the shear modulus of the elastomer. By adopting a LB

value of G_{LB}=0.77MPa [10], D_b=0.75m and t_R=0.165m were specified. Assuming that ξ_e=5% is provided by the elastomer of LDRBs ($c_e=4\pi m\xi_e/T_p$), the LB damping coefficient of LVDs was defined by considering ξ_d= 20% and equating the energy/cycle of the 4 dampers to the energy/cycle of the single damper as $c_{d,LB}=(4\pi m\xi_d/T_p)/4$=639 kN/(m/s) (i.e. per damper). In the case of NLVDs, substituting u_0=0.240 (Table 2) and a=0.2 in Eq. (3) resulted in $c_{d,LB}$=355 kN/(m/s)$^{0.2}$. UB-DPs were calculated based on the previous properties of devices and G_{UB}=1.12MPa [10], $c_{d,UB}=1.35c_{d,LB}$ (i.e. ±15% variability of the nominal c_d).

Shear forces per abutment and pier (V_i) shown in Step 1 of Table 3 were calculated according to Eq. (5) below that assumes a rigid horizontal movement of the deck and accounts for both the elastic and hysteretic part (if any) of the isolator (1st term), and the damping forces due to the elastomer of the isolators and the VDs (2nd term). In the same equation n_b represents the number of isolators per pier and abutment (i.e. 2) and $n_{p,abt}$ the total number of bridge piers and abutments (i.e. 4). Use of UB shear forces along with estimated values for h_{eq} of pier columns (based on preliminary analysis) within the procedure described in [9] provided an estimate for the required pier strength associated with an allowable 'serviceability'-related concrete strain (i.e. 3.5~4.0‰). Table 3 summarises the adopted reinforcement ratio ρ_l and the corresponding pier yield moments (M_y) defined through M-φ analysis carried out using RCCOLA.NET [26] and considering a minimum transverse mechanical reinforcement ratio (ρ_w) for limited ductile bridges [10]. A reduction of ρ_l demand in the piers of the bridge equipped with NLVDs consistent with the minor reduction of the base shear (~2%) was observed.

$$V_i = n_b\left(V_{b0,i}+k_{bp,i}u_0\right)+\left(m\ddot{U}-\sum_{i=1}^{4}n_b\left(V_{b0,i}+k_{bp,i}u_0\right)\right)\Big/n_{p,abt} \tag{5}$$

In Step 2, eligible records were selected from the PEER NGA-West2 database [27] excluding records containing long velocity pulses. The preliminary search criteria used were moment magnitude of M_w=6.5~7, closest distance to the ruptured area R_{rup}=20~40 km, and average shear wave velocity $V_{s,30}$=180~360 m/s (ground type C) [16]. The sample of eligible events was further constrained by assessing the similarity of spectra of the selected records to the target spectrum over the period range of (0.2~1.5)T_{eff} [10] quantified by the mean-squared-error (*MSE*) of the differences between the spectral accelerations (S_a) of the record and the target spectrum (http://ngawest2.berkeley.edu/). A suite of 7 eligible pairs of records was finally selected resulting in the spectral matching depicted in Fig. 5 for EQIII. Using the H2 components [27], each record was initially scaled to minimise MSE by applying a local (i.e. record-specific) scaling factor SF_i. Subsequently, the ensemble spectrum was scaled by a global SF=1.15 so that it was not lower than 0.9 times the target spectrum over the period range of interest [9], [16].

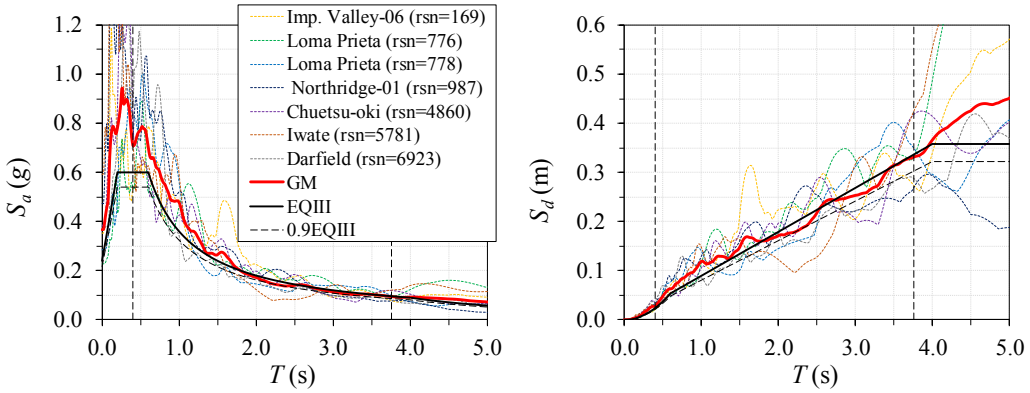

Figure 10: Spectral matching of the scaled median (GM) response acceleration (left) and displacement (right) spectrum to the EQIII (PGA of 0.21g) target spectrum for a suite of natural recordings.

A PIM of the structure was subsequently set up; the strength and stiffness of pier columns were modelled using the modified Takeda hysteresis model (α=0.5, β=0) whereas elastic springs were used to model LDRBs [25], in line with the output of Step 1. The system damping matrix was assembled from the damping matrices of the different subsystems [5]; a tangent stiffness proportional damping matrix [28] was adopted for the structural members of the bridge, whereas dashpot members were used to model viscous damping resulting from the elastomer of isolators and VDs. NLRHAs were performed under the selected suite of records scaled to the intensity corresponding to EQII (Step 2) and subsequently to EQIII (Step 3); results representing the mean response are given in Table 3. 'Operationality' and 'minimal-damage' verifications included specific limits for γ_q (=u_0/t_R) of LDRBs. Due to the linear response of isolators, the restoring capability was not checked and LB-DPs were adopted under EQII, allowing for an explicit (LB-E) calculation of deformations and strains of the isolation system. Analyses for both schemes under EQIII were based on UB-DPs facilitating an explicit (UB-E) calculation of pier moment demand but requiring an implicit calculation of LB deformations (LB-I) that are critical in checking γ_q. Modification factors equal to $u_{0,LB}/u_{0,UB}$=0.120/0.092 and 0.090/0.066 (see Table 2; EQIII) in the case of the LVD and NLVD schemes, respectively, were used to implicitly estimate LB deformations from UB analysis results. Although not required by the suggested procedure, γ_q calculated by explicitly considering LB-DPs (LB-E) are also provided in Table 3 (in grey). None of the isolation system verifications were found to be critical in Steps 2, 3; similarly, pier strength requirements under EQIII were lower than those of Step 1 (more so in the case of the LVD scheme), hence, it was deemed appropriate to proceed to Step 4 without further modifications.

Analysis under EQIV in Step 4 was carried out in both schemes for UB-DPs, enabling an explicit calculation and verification of the response in the substructure, since during the selection of bearings in Step 1, k_{bp} and D_b (related to $\sigma_{v,max}$) rather than limit state strains were found to control t_R. Shear design yielded the transverse reinforcement ρ_w ratios in piers depicted in Table 3 while the curvature ductility demand (μ_φ) in pier sections was found somewhat lower than the values ($\mu_{\varphi,ls}$) corresponding to ε_{cu}=3.5-4.0‰, thus verifying the target performance set in Step 1 for controlled inelastic response of the substructure. Transverse reinforcement requirements were essentially the same in both schemes resulting in identical steel ratios. UB-DPs were also used to check tensile stresses (σ_t) in isolators [29], while verifications of bearing strains due to vertical compression (γ_c) and lateral deformations (γ_q), along with bearing stability (defined as the ratio of the buckling load under compression and lateral deformation P'_{cr} to the peak compressive force $N_{b,max}$ per bearing) [20], required an implicit estimation of isolator deformations; modification factors (see Table 2; EQIV) equal to 0.240/0.183 (LVD scheme) and 0.240/0.178 (NLVD scheme) were employed in this step.

Isolator strains and stability requirements lay within the adopted limits in both schemes, nevertheless, isolator deformations in the NLVD case were somewhat reduced. The uplift criterion was the most critical especially in the NLVD case where the tensile stresses were found close to the stress corresponding to cavitation [29], noting though, that σ_t included in Table 3 represent the peak (rather than the mean) response recorded during NLRHAs. Attention should be also drawn to the fact that an attempt to reduce t_R aiming to match more closely the strain limits of Table 3 is obstructed by $\sigma_{v,max}$ (i.e. a reduction of t_R requires a reduction of D_b to obtain a target k_{bp}) which does not pose a strict limitation nor is it a code requirement (inasmuch as total strains γ_{tot} lie within allowable limits) but it is considered good common practice and is typically recommended by manufacturers. The required force capacity of LVDs and NLVDs ($N_{d,max}$) was estimated in this step as 652 and 455 kN, respectively, corresponding to a reduction of ~30% due to the introduction of a=0.2; the designer may choose to use more than one dampers per abutment/pier location in order to reduce $N_{d,max}$ without affecting analysis results.

Step	EQ	Scheme / Response	DP	LDRBs + LVDs (a=1.0) Abt1	Pier1	Pier 2	Abt 2	LDRBs + NLVDs (a=0.2) Abt1	Pier1	Pier 2	Abt 2	Design Criterion
1	IV	u (m)	LB	0.240	0.240	0.240	0.240	0.240	0.240	0.240	0.240	
		V (kN)		1132	1132	1132	1132	1132	1132	1132	1132	
		u (m)	UB	0.183	0.183	0.183	0.183	0.178	0.178	0.178	0.178	
		V (kN)		1289	1289	1289	1289	1261	1261	1261	1261	
		ρ_l (‰)		-	4.71	10.08	-	-	4.37	9.41	-	> 2.5
		M_y (kNm)		-	4016	4922	-	-	3955	4813	-	
2	II	γ_q (%)	LB-E	35	34	33	36	33	27	19	21	< 100
3	III	γ_q (%)	LB-I	75	73	70	78	62	57	51	63	100-150
			LB-E	69	68	65	71	56	52	47	53	
		M_y (kNm)	UB-E	-	2917	3250	-	-	3056	3453	-	
4	IV	u (m)	UB-E	0.190	0.177	0.166	0.198	0.182	0.163	0.146	0.182	
			LB-I	0.249	0.232	0.218	0.259	0.245	0.220	0.196	0.245	
		γ_q (%)	LB-I	151	140	132	157	149	133	119	148	< 250
		γ_c (%)		91	213	212	99	92	208	203	98	
		γ_{tot} (%)		241	354	344	256	241	341	322	246	< 700
		$P'_{cr}/N_{b,max}$		6.57	2.79	2.81	6.01	6.46	2.86	2.94	6.08	> 1.10
		u (m)	LB-E	0.229	0.220	0.212	0.236	0.221	0.205	0.195	0.225	
		σ_t (MPa)	UB-E	1.29	-	-	1.55	1.66	-	-	2.00	< 2.2 ($2G$)
		$N_{d,max}$(kN)		633	608	571	652	453	449	447	455	
		V (kN)		1399	1230	1172	1449	1432	1232	1174	1447	
		ρ_w (‰)		-	6.67	6.3	-	-	6.67	6.3	-	> 5.15
		μ_φ		-	4.09	3.20	-	-	3.99	3.26	-	
		$\mu_{\varphi,ls}$		-	≤ 4.4-5.1	≤ 3.6-4.1	-	-	≤ 4.5-5.1	≤ 3.7-4.2	-	ε_{cu} ≤ 3.5-4.0‰
A	II	γ_q (%)	LB-E	37	36	34	38	23	18	13	19	< 100
	III	γ_q (%)	LB-E	73	72	69	76	53	48	43	49	100-150
	IV	u (m)	LB-E	0.242	0.232	0.224	0.250	0.221	0.210	0.200	0.225	
		γ_{tot} (%)		226	348	345	238	209	323	318	217	< 700
		$P'_{cr}/N_{b,max}$		7.48	2.87	2.84	6.84	7.94	3.04	3.02	7.35	> 1.10
		σ_t (MPa)	UB-E	0.97	-	-	1.20	0.74	-	-	0.96	< 2.2 ($2G$)
		$N_{d,max}$(kN)		570	561	532	591	437	436	434	440	
		V (kN)		1391	1230	1172	1447	1320	1175	1125	1401	
		μ_φ		-	4.20	3.20	-	-	3.84	2.95	-	
		$\mu_{\varphi,ls}$		-	≤ 4.4-5.0	≤ 3.5-4.0	-	-	≤ 4.5-5.1	≤ 3.6-4.1	-	ε_{cu} ≤ 3.5-4.0‰

Table 3: Comparative evaluation of Def-BD for two different isolation schemes.

Assessment of the designs was carried out to evaluate the efficiency of the proposed procedure for the three different PLs and the considered range of DP of devices (i.e. LB, UB), accounting for all possible combinations of isolator properties and PLs. Since the primary objective of the assessment was the study of the transverse response of the bridge under a seismic excitation that matches as closely as feasible the 'design excitation' (i.e. the design spectrum), NLRHAs were performed for the suite of artificial records (Fig. 1) used to develop the 'design equations' (Fig. 1), scaled to correspond to the considered PL. The strength and stiffness of pier columns was also updated based on M-φ analyses accounting for the final detailing of pier critical sections. In Table 3, selected results are provided (denoted as Step A) for the two alternative isolation schemes. Regarding the reliability of the design procedure, the design was found safe, in that it satisfied the design criteria associated with each PL; in general, the demand derived from assessment was very close to that derived at the design stage despite the adoption of different suites of records. It is worth noting that the implicit approach, although more conservative (as it ought to be), does not necessarily result in overdesigning members and devices. Furthermore, the fairly close match of deformations derived from design/assessment with those of Step 1, indicates the minor effect of the substructure on the peak response and the efficiency

of Eq. (1) in predicting the response of a system equipped with NLVDs (at least in the case considered in this study); discrepancies are also attributed to minor deck torsional effects, the elimination of which would require devices of different properties at each pier and abutment location, an approach not justified in small-to-moderate bridges. Shear forces (explicitly calculated) were close to the values obtained during design and Step 1.

In summary, both systems exhibited similar performance satisfying all adopted design criteria under the studied PLs with the NLVD scheme resulting in relatively lower isolator and deck displacement demand, lower reinforcement ρ_l ratios in piers (~7%), and lower damper force demand (~30%) while additionally providing a safeguard mechanism against excessive structural velocities by limiting the peak damper forces through their nonlinear force-velocity relationship. Last but not least, both isolation schemes resulted in reductions in pier ρ_l (32% in the LVD and 37% in the NLVD scheme) and ρ_w (43%) within critical regions compared to the design of the T7 Overpass (i.e. 'ductile' pier response [9]), indicating that higher performance objectives adopted in isolated bridges do not necessarily result in higher initial cost of substructure design when the isolation system is quasi-optimally selected.

4 CONCLUSIONS

A deformation-based design procedure for seismically isolated bridges was extended herein to address nonlinear VDs aiming at efficient structural design for multiple PLs, through the control of a broad range of design parameters and the aid of rigorous analysis. A key issue in this extension was the introduction of an iterative application of the 'design equation' used to estimate the inelastic demand during the identification of the critical PL as opposed to the case of LVDs wherein no iterations were required. In any case, no iterative structural analysis is needed in contrast to equivalent linearisation approaches based on effective properties. Further issues addressed involved the realisation of the selected scheme through base isolation and energy dissipation devices accounting for the variability of their DPs and the proper consideration of the intended plastic mechanism of the substructure under the relevant PLs. The validity of the procedure was investigated by applying it to the transverse direction (biaxial excitation is currently under investigation) of a bridge previously used by the authors to develop the DefBD method for 'ductile pier' bridges.

The following conclusions were drawn from the above investigations:

- 'Life-safety' verifications under EQIV governed in general the bridge design in both isolation schemes considered. More specifically, uplift considerations and allowable vertical stresses were found to control the characteristics of the isolators, while the requirement for controlled inelastic response and shear design governed ρ_l and ρ_w reinforcement ratios in piers, respectively. Assessment of the design by NLRHA using suites of records closely matching the design spectrum associated with each PL, revealed that the suggested procedure predicted well the structural response while resulting in safe design, in the sense of respecting the adopted design criteria.
- The introduction of nonlinearity in VDs can effectively reduce their size and set an upper limit in damper force demand without significantly affecting the overall bridge response; a relatively lower seismic demand resulted for the bridge type and seismic scenario considered herein. In addition, both LVD and NLVD schemes resulted in lower pier reinforcement ratios compared to the design for ductile response, indicating that cost reductions in substructure design of optimally selected isolation systems may be able to compensate for the initial cost of the isolation system, thus rendering base-isolation an appealing design alternative.
- NLRHAs of the selected system indicated a minor effect of the nonlinearity of VDs on the peak relative displacements of the isolators and the total accelerations of the superstructure,

allowing for Eq. (1, 2) to provide reliable estimates of inelastic demand. A more thorough investigation on the effect of nonlinearity of VDs on the 'design equations' is currently under investigation.

REFERENCES

[1] M. Palermo, S. Silvestri, L. Landi, G. Gasparini, T. Trombetti, Peak velocities estimation for a direct five-step design procedure of inter-storey viscous dampers. *Bulletin of Earthquake Engineering*, **14**, 599-619, 2016.

[2] D. Cardone, M. Dolce, G. Palermo, Direct displacement-based design of seismically isolated bridges. *Bulletin of Earthquake Engineering*, **7**, 391-410, 2009.

[3] N. Makris, G. Kampas, The engineering merit of the "effective period" of bilinear isolation systems. *Earthquakes and Structures* **4**: 397-428, 2013.

[4] P. Franchin, G. Monti, P.E. Pinto, On the accuracy of simplified methods for the analysis of isolated bridges. *Earthquake Engineering & Structural Dynamics* **30**: 363–382, 2001.

[5] A.K. Chopra, *Dynamics of Structures: Theory and Applications to Earthquake Engineering, 4th Edition*. Prentice Hall, 2012.

[6] K.I. Gkatzogias, A.J. Kappos, Deformation-based design of seismically isolated concrete bridges. *16th World Conference on Earthquake Engineering (WCEE)*, Santiago, Chile, January 9-13, 2017.

[7] C. Christopoulos, A. Filiatrault, *Principles of Passive Supplemental Damping and Seismic Isolation*. IUSS Press, 2006.

[8] A.J. Kappos, S. Stefanidou, A deformation-based seismic design method for 3D R/C irregular buildings using inelastic dynamic analysis. *Bulletin of Earthquake Engineering*, **8**, 875-895, 2010.

[9] K.I. Gkatzogias, A.J. Kappos, Deformation-based seismic design of concrete bridges. *Earthquakes & Structures*, **9**, 1045-1067, 2015.

[10] CEN, *Eurocode 8: Design of Structures for Earthquake Resistance - Part 2: Bridges*. CEN, Brussels, Belgium, 2005.

[11] M.C. Constantinou, J.K. Quarshie, *Response Modification Factors for Seismically Isolated Bridges*. MCEER, NY, USA, Report 98-0014, 1998.

[12] M.F. Vassiliou, A. Tsiavos, B. Stojadinović, Dynamics of inelastic base-isolated structures subjected to analytical pulse ground motions. *Earthquake Engineering & Structural Dynamics*, **42**, 2043–2060, 2013.

[13] J.A. Inaudi, J.M. Kelly, Optimum damping in linear isolation systems. *Earthquake Engineering & Structural Dynamics*, **22**, 583–598, 1993.

[14] K.L. Ryan, A.K. Chopra, Estimation of seismic demands on isolators based on nonlinear analysis. *Journal of Structural Engineering*, 130, 392-402, 2004.

[15] Seismosoft, *SeismoArtif - A Computer Program for Generation of Artificial Accelerograms*. [www.seismosoft.com], 2016.

[16] CEN, *Eurocode 8: Design of Structures for Earthquake Resistance - Part 1: General Rules, Seismic Actions and Rules for Buildings*. CEN, Brussels, Belgium, 2004.

[17] J.C. Ramallo, E.A. Johnson, B.F. Spencer, 'Smart' base isolation systems. *Journal of Engineering Mechanics*, **122**, 1088-1099, 2002.

[18] W-H Lin, A.K. Chopra AK, Earthquake response of elastic SDF systems with non-linear fluid viscous dampers. *Earthquake Engineering & Structural Dynamics* **31**, 1623–1642, 2002.

[19] M.N. Fardis, B. Kolias, A. Pecker, *Designer's Guide to Eurocode 8: Design of Bridges for Earthquake Resistance EN 1998-2*. ICE Publishing, 2012.

[20] M.C. Constantinou, I. Kalpakidis, A. Filiatrault, R.A. Ecker Lay, *LRFD-Based Analysis and Design Procedures for Bridge Bearings and Seismic Isolators*. MCEER, NY, USA, Report 11-0004, 2011.

[21] C.P. Katsaras, T.B. Panagiotakos, B. Kolias, Restoring capability of bilinear hysteretic seismic isolation systems. *Earthquake Engineering & Structural Dynamics*, **37**, 557–575, 2008.

[22] D. Cardone, G. Gesualdi, P. Brancato, Restoring capability of friction pendulum seismic isolation systems. *Bulletin of Earthquake Engineering*, **13**, 2449-2480, 2015.

[23] A. Mori, P.J. Moss, A.J. Carr, N. Cooke, Behaviour of laminated elastomeric bearings. *Structural Engineering & Mechanics*, **5**, 451-469, 1997.

[24] G. Weatherill, H. Crowley, L. Danciu, *Preliminary Reference Euro-Mediterranean Seismic Hazard Zonation*. Deliverable 2.7, SHARE Project, 2013.

[25] A.J. Carr, *Ruaumoko 3D: Inelastic Dynamic Analysis Program*. University of Canterbury, New Zealand, 2004.

[26] A.J. Kappos, G. Panagopoulos, RCCOLA.NET - *A Program for the Inelastic Analysis of Reinforced Concrete Cross Sections*. Aristotle University of Thessaloniki, Greece, 2011.

[27] D.T. Ancheta *et al*., *PEER NGA-West 2 Database*. PEER, CA, USA, Report 2013/03, 2013.

[28] D. Pant, A. Wijeyewickrema, M. ElGawady, Appropriate viscous damping for nonlinear time-history analysis of base-isolated reinforced concrete buildings. *Earthquake Engineering & Structural Dynamics*, **42**, 2321–2339, 2013.

[29] CEN, *Antiseismic devices (EN15129)*. CEN, Brussels, Belgium, 2009.